Materials Research. 2022; 25:e20210428
DOI: https://doi.org/10.1590/1980-5373-MR-2021-0428

Dielectric Properties of Steatite Ceramics Produced from Talc and Kaolin Wastes

Eliandra Dantas de Araujo[a], Karina Ruiz Silva[a]*, João Paulo de Freitas Grilo[b], Daniel Araújo de Macedo[c], Lisiane Navarro de Lima Santana[a], Gelmires de Araújo Neves[a]

[a]Universidade Federal de Campina Grande, Unidade Acadêmica de Engenharia de Materiais, 58429-900, Campina Grande, PB, Brasil.
[b]Universidade de Aveiro, Departamento de Engenharia de Materiais e Cerâmica, 3810-193, Aveiro, Portugal.
[c]Universidade Federal da Paraíba, Departamento de Engenharia de Materiais, 58051-900, João Pessoa, PB, Brasil.

Received: August 24, 2021; Revised: December 02, 2021; Accepted: March 15, 2022

The main objective of this work was to study the use of kaolin processing wastes in the production of steatite ceramics, emphasizing mechanical strength and dielectric properties. Steatite ceramics were prepared using mixtures of talc with fine and coarse particle kaolin wastes (7.5, 10 and 12.5 wt.%) sintered at different temperatures (1200, 1250 and 1300°C). After sintering, the specimens were submitted to mineralogical and microstructural characterization. Linear shrinkage, apparent porosity, flexural strength and dielectric properties were also evaluated. Results showed the formation of the crystalline phases protoenstatite and quartz for all produced ceramics. The results verified for porosity, mechanical strength and dielectric properties proved to be suitable for the application of this material in electrical insulation.

Keywords: *Protoenstatite, dielectric properties, electrical insulators.*

1. Introduction

Steatite ceramics are materials based on magnesium metasilicate, which is one of the main components of the ternary system $MgO\text{-}Al_2O_3\text{-}SiO_2$. They are mainly composed of enstatite phase ($MgSiO_3$), which has density of 3.21 g/cm^3, melting point of 1557°C and orthorhombic crystalline structure[1]. Enstatite occurs in three stable polymorphic forms: protoenstatite, clinoenstatite and orthoenstatite[2]. The characteristics of these ceramics include low dielectric constants and dielectric losses, high temperature resistance and high mechanical strength[3,4]. They are usually used for applications such as gas burners, heating element supports, coatings for thermostats, electrical panels and insulators[5,6].

In general, steatite ceramics are produced from natural raw materials, and it is very common to use mixtures of talc and plastic clays[6,7]. Each raw material has an important role in the processing of these ceramic materials: talc is responsible for being a precursor source of the protoenstatite phase during sintering, and clay facilitates the molding and processing of the ceramic mass[8,9].

Kaolin is a material rich in clay, used in various industry segments: paper, ceramics, rubber, plastics, pharmaceuticals, paints and cosmetics. The kaolin group minerals have a 1:1 basic layer structure, with tetrahedral silica and octahedral alumina layers, and their composition is expressed by the chemical formula $Al_2Si_2O_5(OH)_4$[10]. In order to be used in industry kaolin must be subjected to a series of processes that generate a large amount of wastes from this raw material[11]. The waste generated during the first kaolin processing stage is mainly composed of coarse particles (basically consisting of quartz), being called "coarse waste". In the second processing stage, in which the kaolin is purified, a fine particle waste is generated, commonly called "fine waste"[12]. Generally, all these wastes are improperly disposed in nature, causing damage to fauna and flora, and to the population health[13,14]. In this sense, kaolin processing wastes have been studied and shown a great potential to be incorporated in masses for ceramic products manufacturing[15-20]. However, it should be noted that there are no studies in the literature on the use of these wastes for application in electrical ceramics. The use of kaolin wastes as an alternative raw material by the ceramic industry can contribute to the reduction of environmental impacts generated by their improper disposal in nature. Thus, it is extremely important to develop studies that assess the feasibility of using these wastes.

In recent years, several studies have been carried out on the production of steatite ceramics from natural and synthetic raw materials, emphasizing mineralogical and dielectric properties[3,7,21-25]. The dielectric constant is one of the main parameters that is observed for the technological point of view. Values around 5-7 are typically observed for steatite-based ceramics[6,9,26,27].Generally, talc and kaolinitic clay are used as raw materials for the production of steatite ceramics with dielectric properties. However, there is little research on the incorporation of solid waste in the composition of ceramic masses for this purpose[28] and there are no studies on the use of kaolin waste. In this context, the objective of this work was to investigate the dielectric behavior of

*e-mail: karinaruizsilva@gmail.com

steatite ceramics prepared from formulations containing talc and kaolin wastes, sintered at different temperatures. This is an innovative and promising research, making it possible to add value to the waste, which could become a raw material for another industrial sector, allowing for an efficient and sustainable recycling process, with an ecological and economic focus.

2. Experimental Procedures

The raw materials used in this study were talc (purchased from ARMIL Minério S.A), fine and coarse particle kaolin wastes. The kaolin starting powders were obtained from Caulisa S.A, located in Juazeirinho-PB, Brazil. Firstly, kaolin wastes were milled and sieved. This step was adopted to obtain homogeneous granulometry of starting powders. Then, kaolin processing wastes and talc were used to prepare steatite ceramics. These raw materials were chosen due the high content of MgO, and SiO_2 and Al_2O_3, respectively, which are used as source for the formation of protoenstatite ($MgSiO_3$), the main phase in steatite ceramics. Talc and kaolin wastes were ball milled for 3h at approximately 123 RPM with 6 wt.% of humidity. The formulations were prepared using the percentages of 87.5, 90.0 and 92.5 wt.% of talc and 12.5, 10.0 and 7.5 wt.% of kaolin wastes (fine or coarse). For the sake of simplicity materials were labeled according to the type and content of kaolin wastes, namely 7F, 10F and 12F for materials prepared with 7.5, 10 and 12.5 wt.% of fine kaolin waste and 7C, 10C and 12C for those prepared with coarse kaolin waste. The composition (wt.%) of each formulation is detailed in Table 1.

Rectangular bodies (5.0 x 1.5 x 0.5 cm) were shaped by uniaxial pressing at 20 MPa, using a Servitech CT-335 uniaxial hydraulic press. The resulting test specimens were oven-dried at 110°C for 24 hours and then fired at 1200, 1250 and 1300°C for 60 and 120 minutes with heating rate of 5°C/min.

Chemical characterization of starting powders was performed by X-ray fluorescence (XRF), using a Shimadzu EDX-720 energy dispersive X-ray fluorescence spectrometer, under nitrogen atmosphere (N_2). Mineralogical characterization was carried out by X-ray diffraction (XRD), using a Shimadzu Lab XRD-6000 X-ray diffractometer equipped with a Cu-Kα radiation tube, operating at a 2θ scan angle of 5-60º, scan speed of 2º/min and step size of 0.02º. Crystalline phases were identified and quantified using the JCPDS powder diffraction files contained in the PC-PDFWIN database of the Shimadzu XRD-6000 package software. Particle size distribution was estimated by granulometry using a Cilas 1064-LD particle size analyzer.

Mechanical strength tests of sintered bodies were performed using a Shimadzu Autograph AG-X universal test machine, equipped with a Shimadzu load cell with a capacity of 50 kN, operating at 0.5 mm/min speed of applied force.

Subsequently, the ceramic bodies were subjected to a microstructural analysis by scanning electron microscopy (SEM), using a TESCAN Vega3 microscope, in the secondary electrons mode.

The electrical performance of ceramic bodies was tested by impedance spectroscopy. Tests were performed at room temperature and from 400 to 800°C in air using a Hewlett Packard 4284A LCR meter in a two-probe configuration (frequency range from 20 Hz to 1 MHz with a voltage amplitude of 0.5 V). Au electrodes were painted on the parallel faces of the samples and thermally treated at 800°C for 15 min. Electrical conductivity (σ), dielectric constant (εr) and dielectric loss (tan δ) were determined using the following Equations 1-3:

$$\sigma = \frac{d}{A\,R} \tag{1}$$

$$\varepsilon_r = \frac{C\,d}{\varepsilon_0\,A} \tag{2}$$

$$\tan\delta = \frac{\varepsilon}{\varepsilon_r}\,,\quad \varepsilon = \frac{d}{(2\pi f)A\,\varepsilon_0}\frac{Z'}{Z'^2 + Z''^2} \tag{3}$$

where d and A are the thickness and cross-section area of the ceramic sample, respectively. R is the total ohmic resistance of the sample, obtained from the impedance spectra by assuming the intercept of the real axis (Z) at low frequency; f is the frequency in Hz; C is the capacitance in pF; ε_r and ε_0 (8.854×10^{-12} F/m) are the dielectric constant and dielectric permittivity in vacuum, respectively. Z' and Z'' are the real and imaginary parts of impedance, respectively. The frequency-dependent capacitance was estimated using the equation for the impedance of a capacitor (Equation 3), considering Zc=Z''. The activation energy (E_a) for the conduction process can be directly calculated from the conductivity values (σ) using the following Arrhenius-type equation (Equation 4):

$$\sigma T = \sigma_0 \exp(-E_a / RT) \tag{4}$$

where σ_0 is a pre-exponential factor, T is the measured temperature (in Kelvin) and R is the gas constant.

3. Results and Discussion

The assessment of chemical characteristics of powders is essential to have controlled variables during ceramic processing.

Table 1. Composition (wt.%) of the formulations.

Raw Material	Formulations					
	7F	10F	12F	7C	10C	12C
Talc	92.5	90.0	87.5	92.5	90.0	87.5
Fine kaolin waste	7.5	10.0	12.5	-	-	-
Coarse kaolin waste	-	-	-	7.5	10.0	12.5

In Table 2 the chemical composition of starting materials is shown. Talc presented SiO_2 and MgO as its major oxides, which come from the tetrahedral and octahedral layers of its crystalline structure. Both kaolin wastes presented high SiO_2 and Al_2O_3 contents with different SiO_2/Al_2O_3 content ratio. While the fine kaolin waste has SiO_2/Al_2O_3 content ratio of 1.22, the coarse waste has 2.47.

Chemical composition of the formulations containing kaolin wastes is described in Table 3. The high contents of SiO_2 and MgO observed for all compositions are mainly related to talc ($Mg_3(Si_4O_{10})(OH)_2$). The SiO_2 content is also associated with the structure of kaolinite and mica, as well as with quartz in the form of free silica[29]. Additionally, it is observed that the SiO_2 content was higher for the compositions containing coarse kaolin waste, probably due to the presence of a greater amount of free silica in this waste. Fluxing oxides (K_2O, Fe_2O_3 and CaO) were also identified (< 1%), which are probably associated with accessory minerals or impurities. The contents of SiO_2 (from approximately 56 to 70%), MgO (from 22 to 27%) and Al_2O_3 (from 2 to 7%) verified are similar to those found by Terzic et al.[9] and Soykan et al.[22], who studied ceramic masses for steatite ceramics production.

Table 4 shows the values of average particle size of starting materials. The previous adopted processing conditions (described in the section 2) were used to ensure a more reliable average particle size. In fact, particle size observed for the coarse waste is at least 50% larger in comparison to fine waste. The average diameters (D_a) observed for talc, and for fine and coarse kaolin wastes were, respectively, 5.45 μm, 22.11 μm and 33.83 μm.

XRD acquisition (not shown here) was performed for the starting materials. It was found that talc is mainly composed of the crystalline phases talc (JCPDS 29-1493) and quartz (JCPDS 46-1045), while both kaolin wastes are composed of kaolinite (JCPDS 89-6538), mica (JCPDS 83-1808) and quartz (JCPDS 46-1045) phases. Figure 1 shows the XRD spectra of the ceramics produced from the compositions a) 7F, b) 10F, c) 12F, d) 7C, e) 10C and f) 12C, sintered at the temperatures of 1200 and 1300°C for 60 minutes. The presence of two crystalline phases is observed in all XRD spectra: protoenstatite (JCPDS 74-0816) and quartz (JCPDS 46-1045), phases similar to those observed by Soykan[22] and Urtekin et al.[5]. Protoenstatite is a polymorph of the enstatite phase, originated from the talc deoxydrilation during heating, and is stable at temperatures between approximately 1000°C and 1300°C[30,31]. According to Mielcarek et al.[31], quartz is undesirable in steatite ceramics, but it can occur in small amounts.

Table 5 shows the quantification of the crystalline phases of ceramic bodies after heat treatment at temperatures of 1200 and 1300°C for 60 minutes. For all formulations it was found that quartz phase decreased considerably according to the increase of sintering temperature, while the protoenstatite phase

Table 2. Chemical composition (% wt.) of the raw materials.

Oxides	Talc	Fine kaolin waste	Coarse kaolin waste
SiO_2	62.0	43.4	63.4
Al_2O_3	1.5	35.6	25.7
MgO	26.2	1.1	0.8
K_2O	0.1	1.6	1.3
Fe_2O_3	0.2	0.6	0.8
CaO	0.2	-	-
Others	0.1	0.2	0.8
LOI*	9.8	17.6	7.1

*Loss on ignition at 1000°C.

Table 3. Chemical composition (% wt.) of formulations containing fine (7F, 10F and 12F) and coarse (7C, 10C and 12C) kaolin wastes.

Oxides	7F	10F	12F	7C	10C	12C
SiO_2	58.8	56.0	57.4	63.2	62.7	64.8
Al_2O_3	3.4	5.5	6.9	5.5	4.3	4.8
MgO	23.4	21.2	21.6	25.0	24.2	24.6
K_2O	0.2	0.3	0.3	0.2	0.2	0.2
Fe_2O_3	0.3	0.3	0.3	0.2	0.3	0.3
CaO	0.2	0.2	0.2	0.2	0.2	0.2
Others	-	0.1	0.1	0.2	-	0.3
LOI*	13.8	16.5	13.2	5.5	8.1	4.9

*Loss on ignition at 1000°C.

Table 4. Particle size distribution of raw materials.

Raw Material	D_a (μm)	D_{10} (μm)	D_{50} (μm)	D_{90} (μm)
Talc	5.45	0.86	3.77	13.18
Fine kaolin waste	22.11	1.79	19.02	47.31
Coarse kaolin waste	33.83	2.96	32.20	67.12

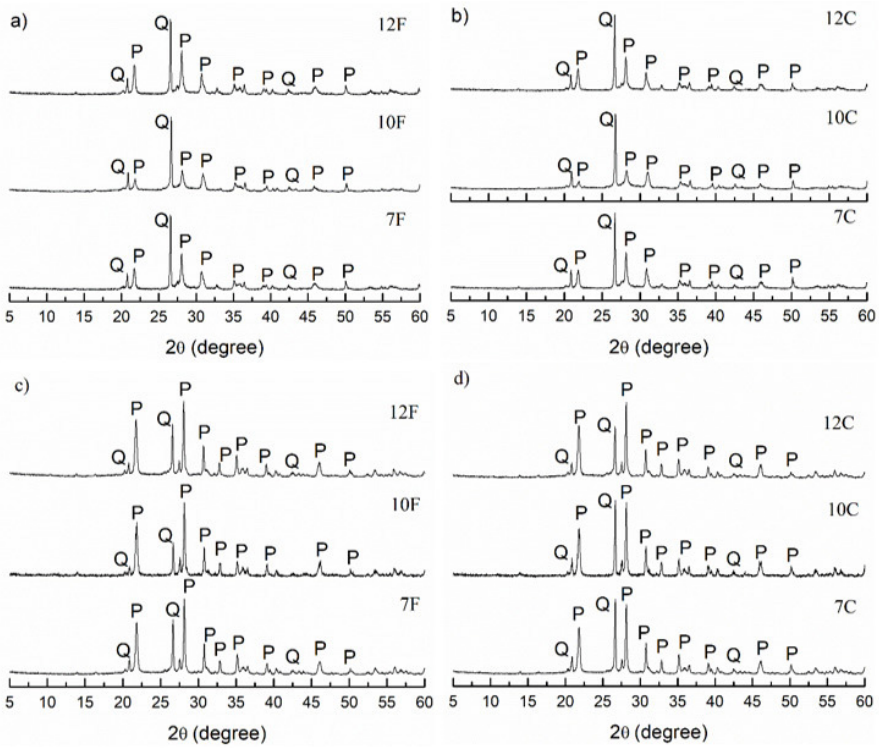

Figure 1. Normalized XRD spectra of the ceramic bodies produced from the formulations containing fine (7F, 10F and 12F) and coarse (7C, 10C and 12C) kaolin wastes, and sintered at temperatures of 1200 and 1300°C for 60 minutes. Q – Quartz; P – Protoenstatite.

Table 5. Quantification of crystalline phases of ceramic bodies after heat treatment at temperatures of 1200 and 1300°C for 60 minutes.

Formulation	Protoenstatite	Quartz	Amorphous phase
7F-1200°C	48.5	38.8	12.7
10F-1200°C	35.2	54.7	10.1
12F-1200°C	53.7	34.9	11.4
7C-1200°C	52.6	41.3	6.2
10C-1200°C	33.7	58.1	8.2
12C-1200°C	51.2	41.3	7.6
7F-1300°C	75.9	18.0	6.1
10F-1300°C	72.1	10.7	17.2
12F-1300°C	76.0	17.4	6.6
7C-1300°C	70.6	25.4	4.0
10C-1300°C	64.7	23.6	11.7
12C-1300°C	75.0	17.4	7.6

increased, evidencing the preferable formation of this phase in the presented systems. This behavior is more pronounced for formulations containing fine kaolin waste, which presents a higher SiO_2/Al_2O_3 ratio (Table 2) compared to coarse waste. Probably, the smaller amount of SiO_2 in the form of free silica present in the fine waste, as well as its smaller particle size, may have influenced the reaction kinetics. Smaller quartz particles dissolve in the glass phase more easily during sintering than large particles, due to their greater surface area.

Figure 2 shows the linear shrinkage as a function of sintering temperature and dwell time for the formulations containing a) fine and b) coarse kaolin waste. The shrinkage of ceramic bodies is associated with the densification process, favored by the greater packing of the particles and the larger contact area between them, as well as the formation of a liquid phase during heating due to the presence of fluxing oxides present in the starting materials.

Lower linear shrinkage values are observed for formulations containing coarse kaolin waste than for those with fine waste. This behavior is verified for all studied sintering conditions, and is due to the larger particle size of the coarse waste and also its higher quartz content, in comparison with the fine waste. Coarser particles result in a smaller contact area, compromising the reactivity during sintering and, consequently, disfavoring the densification of the sintered bodies. Generally ceramics with a greater amount of quartz have lower linear shrinkage[32].

Figure 3 describes the behavior of apparent porosity as a function of sintering temperature and dwell time for the formulations containing a) fine and b) coarse kaolin waste. It is verified that the apparent porosity for all studied formulations decreased according to the increase in sintering temperature and dwell time. These results corroborate with those obtained for linear shrinkage (Figure 2), that is, the increase in temperature and dwell time favor the filling of pores by the liquid phase and the consequent densification of the bodies. Mixtures containing a greater amount of talc had higher porosity values, probably due to the formation of pores resulting from its dehydroxylation during the sintering step[33]. The lowest apparent porosity values presented by the formulations containing fine and coarse wastes were 2.6% (12F-1300°C/120 min) and 7.1% (12C-1300°C/120 min),

respectively. Porosity strongly influences the dielectric constant of insulating ceramic materials[34]. Apparent porosity values observed for ceramics sintered at 1300°C are similar to those found by Wang et al.[25] who investigated steatite ceramics from synthetic and natural raw materials.

Figure 4 shows the flexural strength as a function of sintering temperature and dwell time for the formulations containing a) fine and b) coarse kaolin waste. It is observed that flexural strength increased significantly with increasing sintering temperature and dwell time. This behavior is related to mineralogical and microstructural changes that occur during the sintering process. During heating, talc decomposition produces crystals of protoenstatite and amorphous silica[22,23]. The formation of protoenstatite phase is associated with improved mechanical properties in steatite ceramics[28]. For the studied compositions, the increase in temperature and dwell time favored the formation of a greater amount of liquid phase, providing stabilization and increase in the crystallization rate of the protoenstatite phase (Figure 1), as well as a reduction in the porosity (Figure 3), contributing to the formation of ceramic microstructures with greater mechanical strength. Protoenstatite formed at high temperature, if not stabilized, tends to transform into the polymorph clinoenstatite at room temperature. This transformation is undesirable in steatite ceramics, as it generates intrinsic stresses that induce the formation of cracks in the ceramic body, degrading its mechanical properties[21,31].

The mechanical properties of steatite strongly depend on the temperature cycle used in the synthesis process, largely because enstatite undergoes a complex series of polymorphic transitions[8]. For the studied formulations in this work, only peaks of the polymorph protoenstatite were detected (Figure 1). According to some researchers[21,23,31], generally protoenstatite is stabilized by the glass phase in steatite ceramics, in order to avoid the proto-clinoenstatite transformation.

Higher flexural strength values are verified for the formulations containing fine kaolin waste (reaching 84.1 MPa) compared to those with coarse waste (reaching a maximum of 65.4 MPa), under the same sintering conditions.

Figure 5 shows SEM images of the formulations sintered at 1300°C for 60 minutes. It is revealed the presence of prismatic crystals of protoenstatite (with lengths ranging from approximately 4 μm to 7 μm), surrounded by a

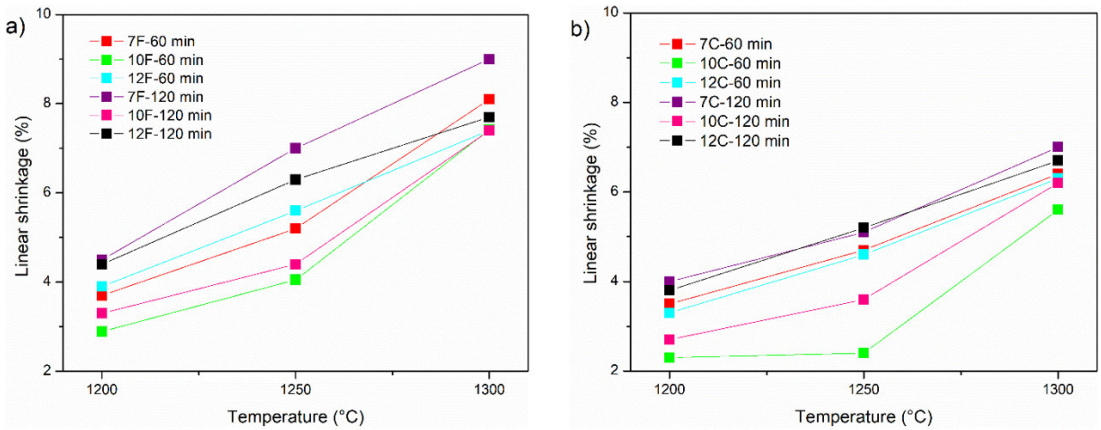

Figure 2. Linear shrinkage (%) as a function of sintering temperature (1200 – 1300°C) and dwell time (60 – 120 minutes) for the formulations containing a) fine and b) coarse kaolin wastes.

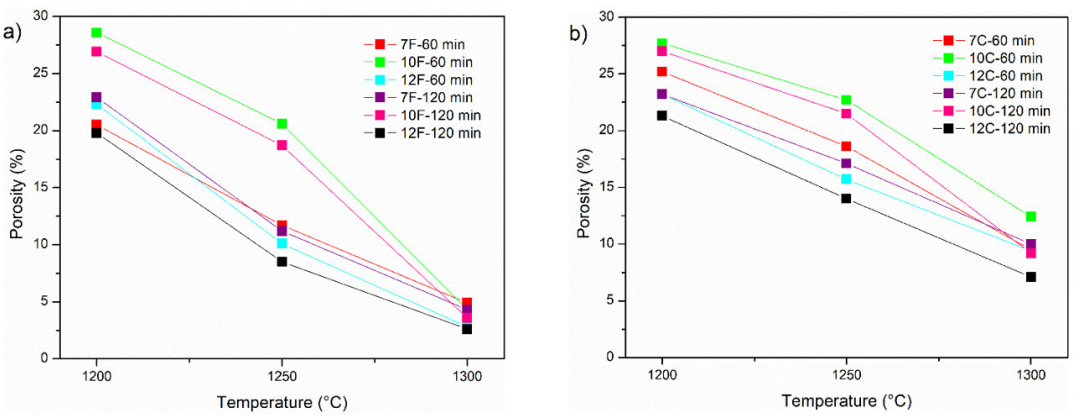

Figure 3. Apparent porosity (%) as a function of sintering temperature (1200 – 1300°C) and dwell time (60 – 120 minutes) for the formulations containing a) fine and b) coarse kaolin wastes.

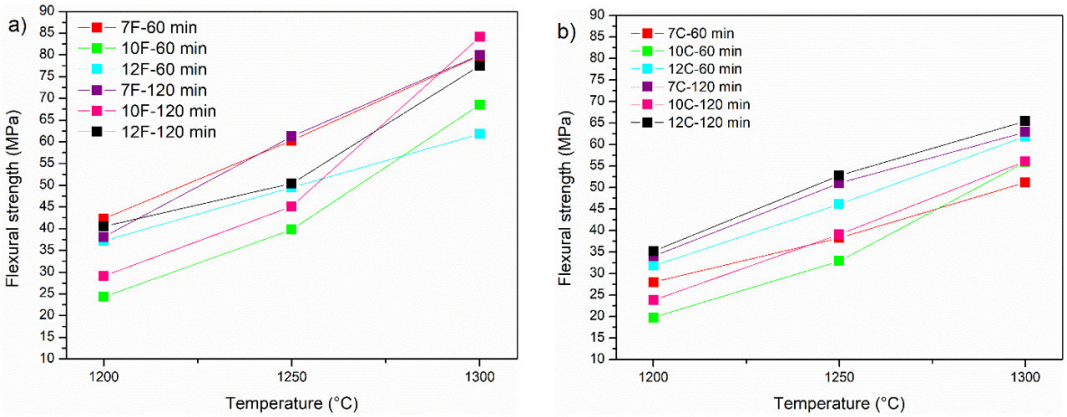

Figure 4. Flexural strength (MPa) as a function of firing temperature (1200 – 1300°C) and dwell time (60 – 120 minutes) for the formulations containing a) fine and b) coarse kaolin wastes.

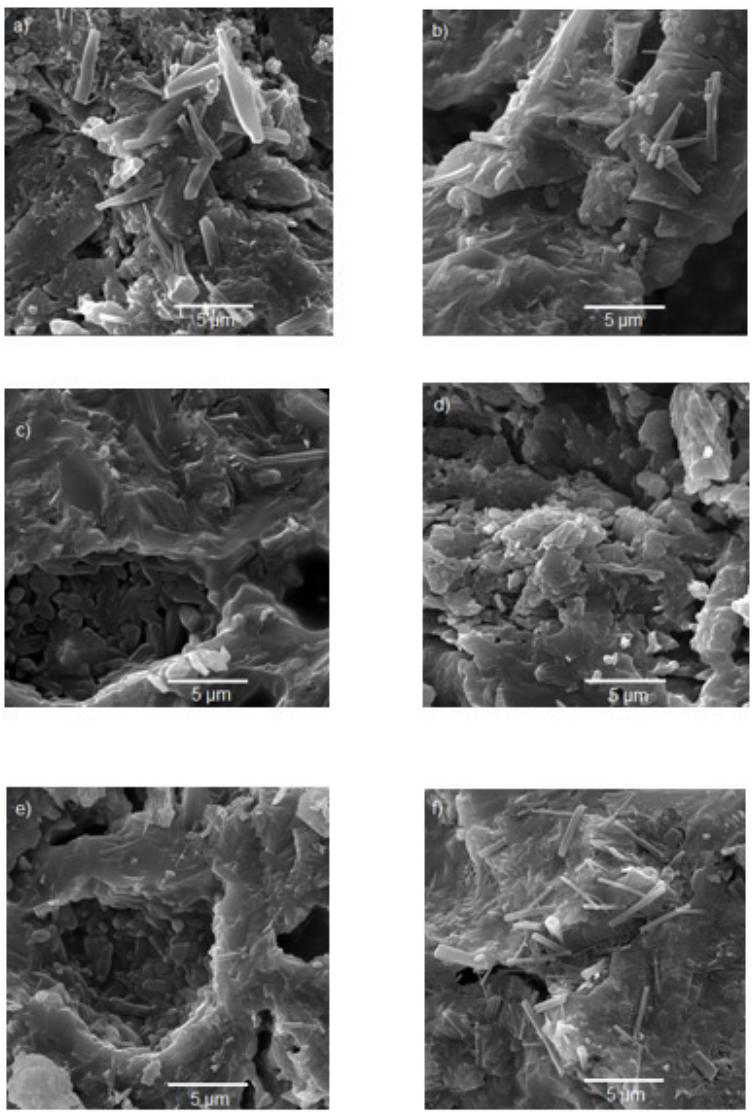

Figure 5. SEM images of the ceramic bodies produced from the formulations a) 7F, b) 10F, c) 12F, d) 7C, e) 10C and f) 12C, and fired at 1300°C for 60 minutes.

vitreous phase and small quartz grains (with diameters of approximately 1 μm), very similar to those already found in literature[9]. For formulations containing the highest waste content, 12F and 12C (12.5 wt.% of fine and coarse kaolin waste, respectively), it is observed a microstructure with a greater amount of vitreous phase compared to the others. The increase in kaolin waste content probably contributed to the formation of a more abundant liquid phase during the sintering process, due to the presence of fluxing oxides in its composition.

Silica from clay dehydroxylation is more reactive than that from talc dehydroxylation. When the sintering temperature increases and the alumina content is higher, liquid phase penetrates the dehydroxylated talc particles leading to a secondary rearrangement. This process leads to a decrease in the average grain size of the crystalline phase, which can improve the material's behavior, as larger grains demonstrate a strong tendency to transform from protoenstatite to clinoenstatite[21].

Impedance spectra, measured at 600°C in air, of the ceramic bodies fired at 1300°C for 60 minutes are shown in Figure 6. It was used the usual representation of the imaginary part (-Z'') versus the real part (Z') of the impedance, and adjustments were made using the geometric factor (sample cross-sectional area divided by its thickness). The spectra present a single arc for each composition, a behavior generally exhibited by materials consisting of glass and crystalline phases, and is due to the dominant contribution of intragranular phenomena[35-37]. These results are in agreement with the microstructure of the studied ceramics, since they consist of protoenstatite crystals immersed in a vitreous phase.

An increase in electrical resistivity is observed for the studied compositions as the kaolin waste content increases, which is probably related to the decrease in porosity (Figure 3).

Figure 7 shows Arrhenius plots of total electrical conductivity, obtained over a temperature range of 400 to 800°C, for samples sintered at 1300°C for 60 minutes. It is observed that the electrical conductivity (σ) of the ceramic bodies increased with increasing temperature for all formulations, as expected. Activation energies, derived from these plots, and electrical conductivity values at 400, 600 and 800°C are listed in Table 6. Activation energies ranged from 94.1 to 96.1 kJ.mol^{-1} for compositions containing fine kaolin waste and from 92 to 93.7 kJ.mol^{-1} for those containing coarse waste. These activation energies are close to those found by Andrade et al.[38] and Silva et al.[19], who studied caramics for electronics-related applications. Regarding electrical conductivity, the compositions containing fine kaolin waste showed higher values.

Figure 8 shows the dielectric constant (ε_r) and dielectric loss (tan δ) as a function of frequency (0-1000 kHz), for all compositions sintered at 1300°C for 60 minutes. It is verified that the values of ε_r and tan δ decreased with increasing frequency. At 1000 kHz, formulations 7F, 10F and 12F

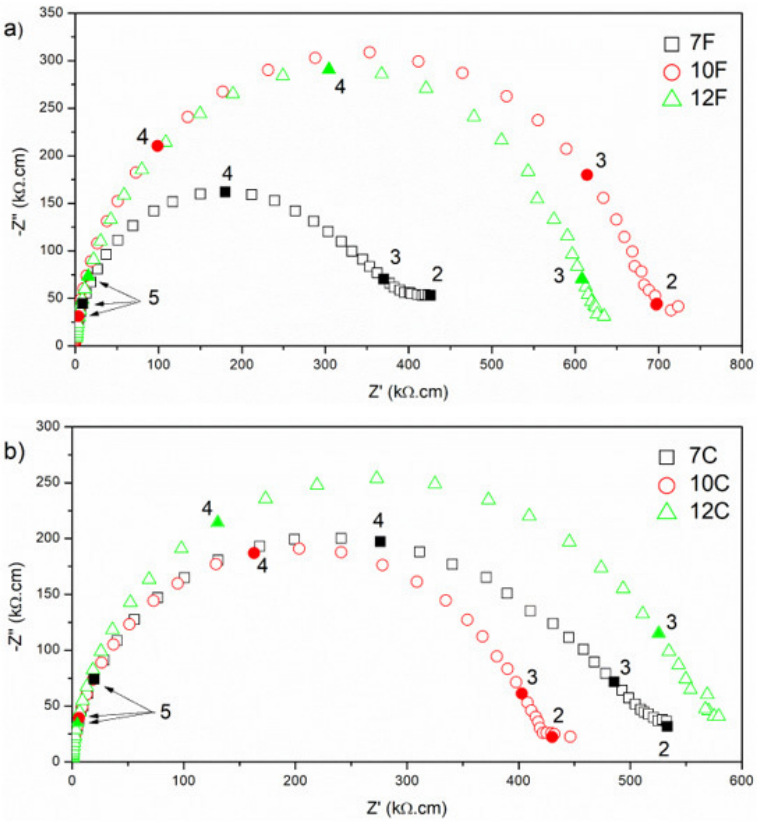

Figure 6. Impedance spectra, measured at 600°C in air, of the ceramic bodies produced from the formulations containing a) fine and b) coarse kaolin wastes, sintered at 1300°C for 60 minutes. The numbers indicate the decade of the frequency.

Table 6. Activation energy (E_a, kJ.mol^{-1}) and electrical conductivity (σ, S.cm^{-1}) of ceramic bodies sintered at 1300°C for 60 minutes.

Amostra	7F	10F	12F	7C	10C	12C
E_a (400-800 °C)	95.2	94.1	96.1	92.0	93.7	92.7
σ (x10^{-8}) a 400 °C	6.96	4.34	3.99	6.90	6.72	5.03
σ (x10^{-6}) a 600 °C	2.76	1.45	1.61	2.18	2.42	1.78
σ (x10^{-5}) a 800 °C	2.52	1.52	1.54	2.06	2.18	1.58

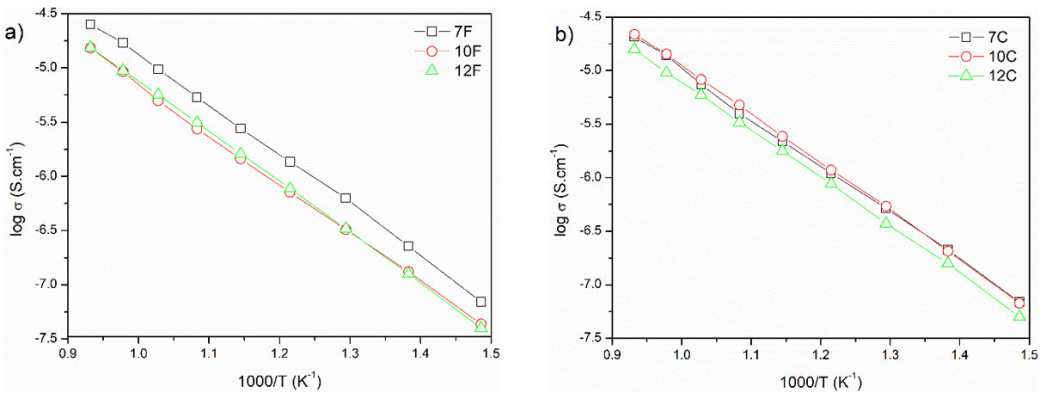

Figure 7. Arrhenius plots of the total electrical conductivity for the formulations containing a) fine and b) coarse kaolin wastes, sintered at 1300°C for 60 minutes.

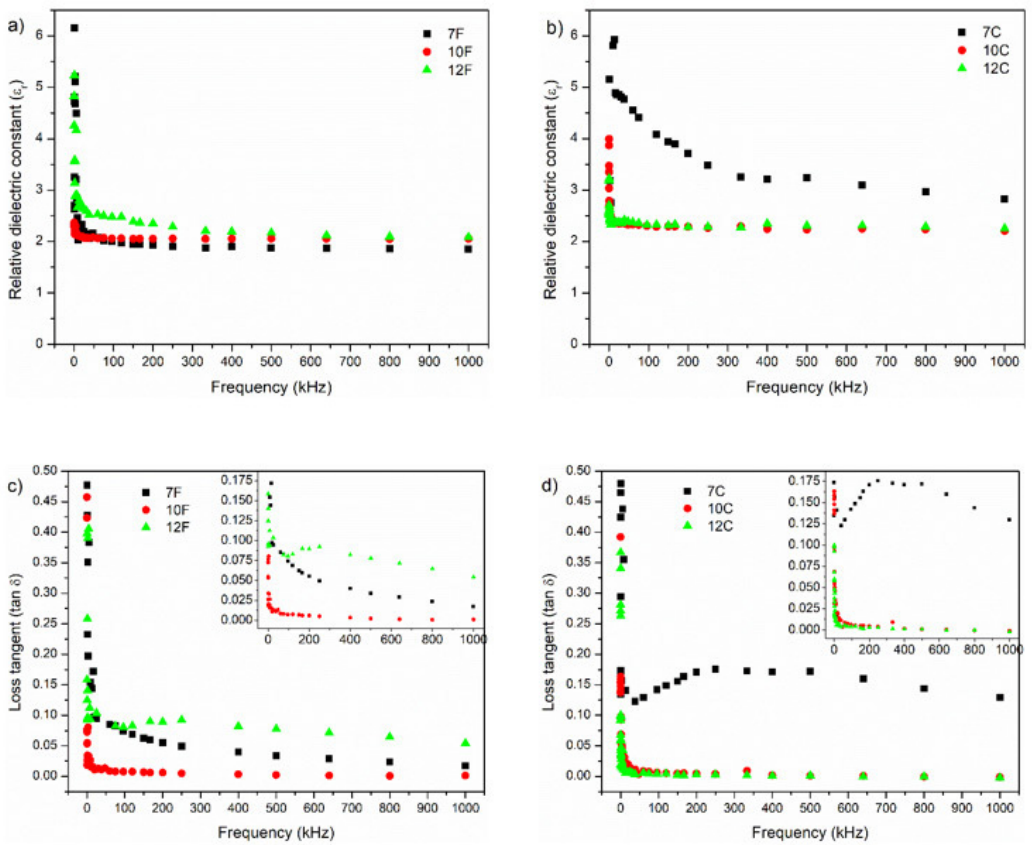

Figure 8. Dielectric constant (ε_r) and dielectric loss (tan δ) as a function of frequency, for the formulations containing a) fine and b) coarse kaolin wastes, sintered at 1300°C for 60 minutes.

exhibited ε_r values of 1.85, 2.05 and 2.09, respectively, and for formulations 7C, 10C and 12C, the values of 2.82, 2.21 and 2.25 were found, respectively. At high frequencies, the dielectric constant may have been influenced by electronic and interfacial polarizations due to the presence of the crystalline phases protoenstatite and quartz. Low dielectric constant value (< 12) is essential for electrical insulation applications[26]. Generally, values of dielectric constant are in the range of 5-7[6,9,26]. The values estimated for the presented ceramics are at least 2-3 times below that those found in literature. Microstructural characteristics, such as porosity across the ceramic volume, can cause these low polarization effects during impedance testing.

At the frequency of 1000 kHz, dielectric losses of 0.017, ~0.001 and 0.054 were observed for the formulations 7F, 10F and 12F, respectively. For 7C, 10C and 12C were found losses of 0.129, ~0.001 and ~0.001, respectively. These values are very similar to those found by Makovsec et al.[6] who studied steatite ceramics produced from natural raw materials. Values of tan $\delta < 0.04$ are suitable for electronics-related applications[39].

4. Conclusions

In this work, the dielectric properties of steatite ceramics produced from talc and kaolin wastes were evaluated. In this sense, it is concluded that all ceramics presented protoenstatite and quartz as major crystalline phases. Regarding the physical-mechanical and electrical properties, the studied compositions are suitable for production of steatite ceramics for use as electrical insulators. The use of wastes as alternative ceramic raw materials can greatly contribute to the environment, reducing the environmental impacts caused by them.

5. Acknowledgments

Authors acknowledge financial support received from CAPES – Brazil (scholarship for Eliandra D. Araujo) and CNPq – Brazil (proc. 306832/2019-4 and 309234/2020-4).

6. References

1. Rohan P, Neufuss K, Matějíček J, Dubský J, Prchlík L, Holzgartner C. Thermal and mechanical properties of cordierite, mullite and steatite produced by plasma spraying. Ceram Int. 2004;30(4):597-603.
2. Lee WE, Heuer AH. On the polymorphism of enstatite. J Am Ceram Soc. 1987;70(5):349-60.
3. Terzić A, Andrić L, Stojanović J, Obradović N, Kostović M. Mechanical activation as sintering pre-treatment of talc for steatite ceramics. Sci Sinter. 2014;46(2):247-58.
4. Valášková M, Zdrálková J, Tokarský J, Martynková GS, Ritz M, Študentová S. Structural characteristics of cordierite/steatite ceramics sintered from mixtures containing pore-forming organovermiculite. Ceram Int. 2014;40(10):15717-25.
5. Urtekin L, Uslan I, Tuc B. Investigation of properties of powder injection-molded steatites. J Mater Eng Perform. 2012;21(3):358-65.
6. Makovše K, Ramšak I, Malič B, Bobnar V, Kuščer D. Processing of steatite ceramic with a low dielectric constant and low dielectric losses. Informacije MIDEM. 2016;46(2):100-5.
7. Gökçe H, Aĝaoĝullari D, Öveçoĝlu ML, Duman İ, Boyraz T. Characterization of microstructural and thermal properties of steatite/cordierite ceramics prepared by using natural raw materials. J Eur Ceram Soc. 2011;31(14):2741-7.
8. Reynard B, Bass JD, Jackson JM. Rapid identification of steatite-enstatite polymorphs at various temperatures. J Eur Ceram Soc. 2008;28(13):2459-62.
9. Terzić A, Obradović N, Stojanović J, Pavlović V, Andrić L, Olćan D. Influence of different bonding and fluxing agents on the sintering behavior and dielectric properties of steatite ceramic materials. Ceram Int. 2017;43(16):13264-75.
10. Schroeder PA, Erickson G. Kaolin: from ancient porcelains to nanocomposites. Elements. 2014;10(3):177-82.
11. Mendonça AMGD, Souza LMC, Lira YC, Souza VF No, Duarte EVN, Nunes CGL, et al. Kaolin waste as an alternative material for the production of soil- cement brick blocks. Braz J Dev. 2021;7(5):44168-78.
12. Anjos CM, Neves GA. Use of kaolin waste for the production of soil-lime blocks. Rev Eletr Mater Process. 2011;6(2):91-6.
13. Menezes RR, Almeida RR, Santana LNL, Neves GA, Lira HL, Ferreira HC. Analysis of the use of kaolin processing waste and granite sawing waste together for the production of ceramic bricks and roo. Ceramica. 2007;53(326):192-9.
14. Azerêdo AFN, Carneiro AMP, De Azerêdo GA, Sardela M. Hardened properties of lime based mortars produced from kaolin wastes. Key Eng Mater. 2014;600:282-96.
15. Silva VJ, Silva MF, Gonçalves WP, Menezes RR, Neves GA, Lira HL, et al. Porous mullite blocks with compositions containing kaolin and alumina waste. Ceram Int. 2016;42(14):15471-8.
16. Alves HPA, Junior RA, Campos LFA, Dutra RPS, Grilo JPF, Loureiro FJA, et al. Structural study of mullite based ceramics derived from a mica-rich kaolin waste. Ceram Int. 2017;43(4):3919-22.
17. Almeida EP, Brito IP, Ferreira HC, Lira HL, Santana LNL, Neves GA. Cordierite obtained from compositions containing kaolin waste, talc and magnesium oxide. Ceram Int. 2018;44(2):1719-25.
18. Sánchez-Soto PJ, Eliche-Quesada D, Martínez-Martínez S, Garzón-Garzón E, Pérez-Villarejo L, Rincón JM. The effect of vitreous phase on mullite and mullite-based ceramic composites from kaolin wastes as by-products of mining, sericite clays and kaolinite. Mater Lett. 2018;223:154-8.
19. Silva VJ, Almeida EP, Gonçalves WP, Nóbrega RB, Neves GA, Lira HL, et al. Mineralogical and dielectric properties of mullite and cordierite ceramics produced using wastes. Ceram Int. 2019;45(4):4692-9.
20. Almeida EP, Carreiro MEA, Rodrigues AM, Ferreira HS, Santana LNL, Menezes RR, et al. A new eco-friendly mass formulation based on industrial mining residues for the manufacture of ceramic tiles. Ceram Int. 2021;47(8):11340-8.
21. Vela E, Peiteado M, García F, Caballero AC, Fernández JF. Sintering behaviour of steatite materials with barium carbonate flux. Ceram Int. 2007;33(7):1325-9.
22. Soykan HŞ. Low-temperature fabrication of steatite ceramics with boron oxide addition. Ceram Int. 2007;33(6):911-4.
23. Ptáček P, Lang K, Šoukal F, Opravil T, Bartoníčková E, Tvrdík L. Preparation and properties of enstatite ceramic foam from talc. J Eur Ceram Soc. 2014;34(2):515-22.
24. Terzić A, Obradović N, Pouchly V, Stojanović J, Maca K, Pavlović VB. Microstructure and phase composition of steatite ceramics sintered by traditional and spark plasma sintering. Sci Sinter. 2018;50(3):299-312.
25. Wang Z, Shi Z, Wang W, Wang S, Han C. Synthesis of $MgSiO_3$ ceramics using natural desert sand as SiO_2 source. Ceram Int. 2019;45:13865-73.
26. Kingery WD, Bowen HK, Uhlmann DR. Introduction to ceramics. New York: Wiley; 1976.
27. Song ME, Kim JS, Joung MR, Nahm S, Kim YS, Paik JH. Synthesis and microwave dielectric properties of MgSiO3 ceramics. J Am Ceram Soc. 2008;91(8):2747-50.

28. Torres HSS, Varajão AFDC, Sabioni ACS. Technological properties of ceramic produced from steatite (soapstone) residues-kaolinite clay ceramic composites. Appl Clay Sci. 2015;112-113:53-61.
29. Sánchez-Soto PJ, Wiewióra A, Avilés MA, Justo A, Pérez-Maqueda LA, Pérez-Rodríguez JL, et al. Talc from Puebla de Lillo, Spain. II. Effect of dry grinding on particle size and shape. Appl Clay Sci. 1997;12(4):297-312.
30. Smyth JR. Experimental study on the polymorphism of entatite. Am Mineral. 1974;59(3-4):345-52.
31. Mielcarek W, Nowak-Woźny D, Prociów K. Correlation between $MgSiO_3$ phases and mechanical durability of steatite ceramics. J Eur Ceram Soc. 2004;24(15-16):3817-21.
32. Nzeukou AN, Fagel N, Njoya A, Kamgang VB, Medjo RE, Melo UC. Mineralogy and physico-chemical properties of alluvial clays from Sanaga valley (Center, Cameroon): suitability for ceramic application. Appl Clay Sci. 2013;83–84:238-43.
33. Chandra N, Agnihotri N, Bhasin S, Khan AF. Effect of addition of talc on the sintering characteristics of fly ash based ceramic tiles. J Eur Ceram Soc. 2005;25(1):81-8.
34. Kuang X, Jing X, Tang Z. Dielectric loss spectrum of ceramic $MgTiO_3$ investigated by AC impedance and microwave resonator measurements. J Am Ceram Soc. 2006;89(1):241-6.
35. Ribeiro MJ, Abrantes JCC, Ferreira JM, Labrincha JA. Predicting processing-sintering-related properties of mullite-alumina ceramic bodies based on Al-rich anodising sludge by impedance spectroscopy. J Eur Ceram Soc. 2004;24(15–16):3841-8.
36. Malki M, Hoo CM, Mecartney ML, Schneider H. Electrical conductivity of mullite ceramics. J Am Ceram Soc. 2014;97(6):1923-30.
37. Grilo JPF, Alves HPA, Araújo AJM, Andrade RM, Dutra RPS, Macedo DA. Dielectric and electrical properties of a mullite/glass composite from a kaolinite clay/mica-rich kaolin waste mixture. Ceramica. 2019;65(373):117-21.
38. Andrade RM, Araújo AJ, Alves HP, Grilo JP, Dutra RP, Campos LF, et al. On the physico-mechanical, electrical and dielectric properties of mullite-glass composites. Ceram Int. 2019;45(15):18509-17.
39. Zhang L, Olhero S, Ferreira JMF. Thermo-mechanical and high-temperature dielectric properties of cordierite-mullite-alumina ceramics. Ceram Int. 2016;42(15):16897-905.

Supplementary material

The following online material is available for this article:

Figure S1 - Normalized XRD spectra of the ceramic bodies produced from the formulations containing fine kaolin waste (7F, 10F and 12F), and sintered at temperatures of 1200, 1250 and 1300°C for 60 and 120 minutes.

Figure S2 - Normalized XRD spectra of the ceramic bodies produced from the formulations containing coarse kaolin waste (7C, 10C and 12C), and sintered at temperatures of 1200, 1250 and 1300°C for 60 and 120 minutes.